International Journal for Housing Science and Its Applications
Publish August 10, 2025. Volume 46, Issue 4 Pages 7619-7632

https://doi.org/10.70517/ijhsa464656

Digital technology-enabled wearable equipment human-machine interaction - dual-dimensional optimization of product design

Fei Li[1,*] and Lin Lu[2]
[1] School of Physical Education, North University of China, Taiyuan, Shanxi, 030051, China
[2] School of Mechatronics Engineering, North University of China, Taiyuan, Shanxi, 030051, China
Corresponding authors: (e-mail: wenzikuaifei@126.com).

Abstract Exoskeleton robots, as a new type of intelligent wearable device, integrate advanced research findings from fields such as mechanics, control, and ergonomics. They enhance human sensory perception and strength, reinforce physical movement capabilities and endurance, and offer extremely broad application prospects in military, civilian, medical, nursing, and emergency response sectors. This paper analyzes the usage requirements of exoskeleton equipment and the design characteristics of existing equipment, combining ergonomics and kinematics theory to propose design elements and strategies. It introduces topological optimization methods into the design phase of exoskeleton equipment, establishing an intelligent sensing system for exoskeletons. The paper conducts exoskeleton wearing experiments on test subjects, combining dynamics and electromyography analysis to evaluate the effectiveness of the exoskeleton. Human-machine compatibility analysis results show that the walking space of the exoskeleton in the sagittal plane can cover the ankle joint movement trajectory of the human body. Kinematic simulation results indicate that after wearing the exoskeleton, the total joint work done during walking and squatting movements decreased by 20.71% and 17.57%, respectively. Surface electromyography results showed that the distribution patterns of the contribution rates of major lower limb muscles changed to some extent after wearing the exoskeleton, with a significant decrease in the overall integral values.

Index Terms exoskeleton wear, smart wearable devices, topological optimization method, simulation experiment

I. Introduction

Driven by the miniaturization of semiconductor technology and the rapid rise of mobile internet technology, smart wearable devices have emerged and are widely applied in fields such as security, disaster management, healthcare, sports, education, and fashion, with wearable devices gradually becoming a trend [1]-[4]. According to relevant data, the global shipment volume of smart wearable devices reached 190 million units in 2024, with the global smart wearable market size reaching 72.1 billion US dollars. With the introduction of Google Glass, wearable devices have garnered increasing attention, and their future development potential is widely recognized [5]. As early as the 1980s, Casio launched a smartwatch that not only displayed the time but could also record musical notes [6]. Over time, with technological advancements, wearable devices have undergone significant transformations, and their functionalities have become increasingly diverse. Allerta, the company behind inpulse, launched the Pebble smartwatch, which, in addition to standard watch functions, can connect to a smartphone to receive text messages and emails, and even utilize the phone's GPS to track walking speed, distance, and other data [7]. Of course, alongside these wearable devices, many other wearable devices have emerged, such as Bluetooth emergency monitoring systems and posture correction devices [8], [9]. As such, the functional characteristics of smart wearable devices lie in combining fashionable ergonomic design with advanced smart electronic technology, transforming network information from a monotonous physical format into a vivid physiological format, integrating individual human information into the network, and shifting from a separation of humans and the network to humans being within the network and the network adapting to human movements, thereby providing an excellent human-machine interaction experience [10]-[12].

With the development of computer miniaturization, sensor miniaturization, and intelligent textile technology, smart devices have truly achieved the goal of being “worn on the body,” significantly expanding human physiological functions. Wearable technology has become one of the hottest technologies, demonstrating unique advantages in the field of weaponry and equipment [13], [14]. First, the individual soldier integrated combat system integrates wearable microcomputers, sensors, reconnaissance imaging equipment, and communication/navigation devices

into individual soldier combat gear, creating a combat equipment system comprising five subsystems: smart helmets, protective gear, weapons, computing/radio equipment, and software. This enhances an individual soldier's comprehensive combat capabilities on the battlefield, including command and communication, navigation and positioning, situational awareness, coordinated actions, and self-protection [15]. Additionally, Reference [16] proposes a lightweight wearable sensing and feedback mechanism-integrated hand-based command system, enabling soldiers to perform intelligence gathering, surveillance, and reconnaissance tasks through human-machine interaction with robots. Reference [17] integrates edge intelligence and battlefield IoT to design a wearable device driven by multi-agent multi-layer sensors for estimating the direction of gunfire using gloves. Reference [18] designed a bulletproof wearable electronic vest capable of sensing armed attacks, reporting gunfire locations, and providing timely injury response. It is constructed using silver-plated conductive yarn to form sensor units, combined with a Velcro system for sensor installation. Literature [19] describes a wearable device supported by a heterogeneous sensor network, which constructs a multi-level fusion framework based on soldiers' behavior, physiology, emotions, fatigue, environment, and location. This device assists soldiers in making scientific decisions, accurate reporting, and evidence collection under resource-constrained conditions.

Second, smart protective gear. Literature [20] describes a battery-powered wearable electromagnetic protective glove designed using sensors, microcontrollers, and wireless technology. It can release powerful electromagnetic capabilities in battlefield or law enforcement environments to resist external harm. Reference [21] developed a wearable life monitor, which is embedded as a sensor in soldiers' clothing or equipment, to monitor soldiers' physiological loads in real time, analyze physiological needs in different scenarios, and achieve military tasks that better align with actual physical stress. It also assists soldiers in combat preparation and enhances their adaptability. Literature [22] integrates metal detection sensors, NEO-6M devices, ThingSpeak cloud servers, and TTGO TCaII to produce a mine-detection shoe for landmine detection. The shoe can accurately obtain landmine location and coordinate data and upload it to the cloud for storage, enabling local and remote alarm indications to inform soldiers to bypass the area.

Thirdly, intelligent exoskeleton systems. Literature [23] demonstrates the application of wearable exoskeleton systems in the military domain to assist soldiers in carrying heavy loads, reduce their own burden, avoid life-threatening situations in extreme environments, and enhance operational flexibility. Literature [24] uses the upper-body exoskeleton system ARCTiC LawE for firearms training, improving the accuracy and precision of typical law enforcement and military live-fire exercises, thereby helping to reduce training costs.

The article first briefly outlines the current state of application of smart wearable technology, then identifies two key design directions for exoskeleton equipment: human-machine coordination design and high strength-to-weight ratio form design. By deeply integrating topological optimization methods into the industrial design process, the article achieves an integrated design of the morphological structure of exoskeleton equipment and ergonomic motion mechanisms. Concurrently, the article conducts a scheme design for the dimensions of wheeled assistive locomotion devices, thereby designing an exoskeleton intelligent sensing system. It introduces feasible sensor solutions and designs different control circuits and circuit hardware implementations for various sensors. The paper evaluates the performance of the exoskeleton through wearable experiments, combined with dynamic simulation and electromyography data analysis. Additionally, the design's exoskeleton sensor system is validated for reasonableness and feasibility using real-time video recording and recognition results comparison—specifically, gait recognition rate. Finally, a rigorous subjective performance evaluation experiment is conducted using an exoskeleton robot comprehensive performance evaluation system, with detailed quantitative evaluations of the experimental prototype's performance metrics.

II. Method

II. A. Weapons and Equipment Applications

With the development of computer miniaturization, sensor miniaturization, and intelligent weaving technology, smart devices have truly achieved the goal of being “worn on the body,” thereby significantly expanding human physiological functions. First, the individual soldier integrated combat system. Represented by the U.S. Army's “Land Warrior” system and “Targeted Individual Soldier Weapon System,” these individual soldier integrated combat systems integrate wearable microcomputers, sensors, reconnaissance imaging equipment, and communication/navigation devices into individual soldier combat gear, creating a combat system comprising smart helmets, protective gear, weapons, and five subsystems—computing/ radio equipment, and software. This enhances an individual soldier's comprehensive combat capabilities on the battlefield, including command and communication, navigation and positioning, situational awareness, coordinated actions, and self-protection. Second, intelligent protective gear. To protect soldiers' lives, Colombia's Lemur Design Studio has developed a smart shoe called “Save One Life.” Its manufacturing principle involves installing metal detectors made from printed circuits in

the sole of the shoe. When the soldier detects a magnetic field reaction from suspected landmines or other large metal objects during patrol, the connected smartwatch will issue a warning, indicating the location of the suspicious object and advising the soldier to bypass it. Intelligent Textiles Ltd. in the UK uses weaving technology to “weave electronic devices into fabric one stitch at a time.” Their “Spirit” smart fabric product provides insulation for the wearer while also offering mobile power supply, data connectivity, and bulletproof protection. Third, smart exoskeleton systems. The US Defense Advanced Research Projects Agency (DARPA) and Harvard University have collaborated to develop the “Soft Exosuit” exoskeleton “machine suit” for individual soldiers. The primary materials are textiles combined with embedded microprocessors, sensors, and portable power sources. By wrapping around the soldier's waist and thighs, it provides additional load-bearing strength and mobility for combat soldiers. Additionally, the U.S. Army Research Laboratory is testing an arm exoskeleton system called “MAXFAS.” This system reduces arm vibration during shooting training, remembers shooting movements, shortens training cycles, reduces ammunition and budget consumption, and assists soldiers in quickly aiming and firing at targets during combat.

II. B. Key points in the design of exoskeleton equipment

II. B. 1) Exoskeleton Design

Exoskeleton mobility technology is an integrated technological system encompassing sensors, actuators, and controllers. For active exoskeleton equipment, reducing motion feedback latency requires addressing sensor efficiency and motion pattern learning, combined with brain-computer interface control and artificial intelligence to improve follow-up feedback and assistive performance. For passive exoskeleton equipment, the assistive mechanisms typically employ elastic energy storage assistive designs, with the primary influence on the wearer's own movement stemming from the energy storage work process and mechanical structural damping.

Whether for active or passive exoskeleton equipment, the close integration of the motion mechanisms with human anatomy and movement patterns is a critical design consideration. Exoskeleton structures compliant with ergonomic standards can effectively reduce the adverse effects of the equipment on the wearer's natural movement and lower the learning curve for using the equipment, thereby enhancing wearing comfort and operational efficiency [25]. Using the 50th percentile of males aged 18–25 as the baseline, adjustments are made to account for military attire and recent increases in population height. Exoskeleton equipment should have corresponding feedback and assistance modes for soldiers' movement states in different environments and combat scenarios, thereby improving equipment adaptability and energy utilization efficiency. By analyzing human gait during walking and running, we can understand the different performance requirements for exoskeleton operation in these two behavioral modes. Human walking gait and running gait are shown in Figures 1 and 2.

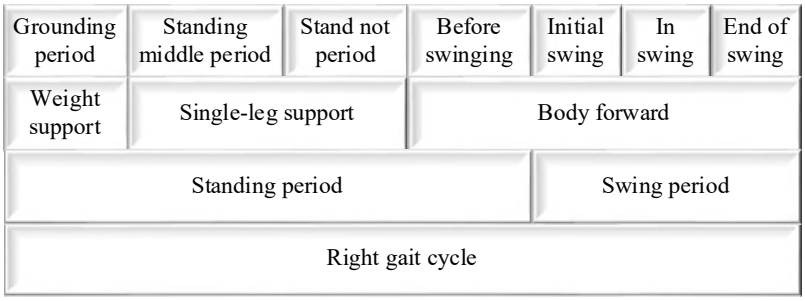

Figure 1: Walking gait cycle

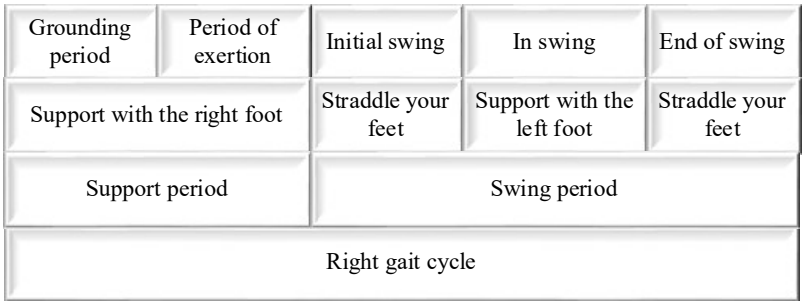

Figure 2: Running gait cycle

II. B. 2) High specific strength airframe design

The weight of the exoskeleton itself remains a burden for the user. The heavier the exoskeleton, the lower its assist efficiency. Therefore, exoskeletons are typically manufactured using high-strength-to-weight ratio materials. Additionally, the structural design of the exoskeleton directly impacts product performance and cost. While ensuring the required strength and stability of the equipment, the exoskeleton structure design should aim to minimize the equipment's self-weight while enhancing assist performance. Lightweight design requires the use of high-strength-to-weight ratio materials and lightweight structures to achieve this. By leveraging the inherent physical properties of materials and structural design, integrated components can be used to consolidate functions such as energy storage, assistance, and support.

II. C. Design Elements and Countermeasures for Exoskeleton Equipment

II. C. 1) Ergonomic motion mechanism and degree of freedom design

1) Chain-type modular back support.

The chain-type modular combination, similar to the human spine, effectively addresses the design requirements for the back components of an exoskeleton, which need to balance load-bearing and mobility functions. The back module is connected to the waist and hip module via hidden hinges on the side that contacts the human body, and the connection method for the back support components is the same. The hinge connection provides freedom of movement for bending actions while maintaining support when the back is straightened [26]. The size of the back module can be significantly adjusted by increasing or decreasing the number of support components, with fine-tuning achieved by adjusting the position of the hinge fixing screws. The back straps are located on the load-bearing components at the position of the latissimus dorsi muscle, close to the human body's natural load-bearing attachment points.

2) Universal joint-type hip joint

Since human hip movement involves multiple directions, using a universal joint can address the practical issues of misalignment and non-coaxiality between the exoskeleton components and limb movements, highly accommodating human freedom of movement and reducing resistance to human movement caused by the equipment. The waist-hip module includes a waist binding component and a hip connection component, connected via a universal joint. Universal joints provide sagittal and coronal plane degrees of freedom while supporting back loads. Since universal joints are the components with the smallest load-bearing area in the entire exoskeleton product, they have high requirements for shear strength. Typically, low-carbon alloy steel treated with carbonitriding or materials with superior performance are considered for manufacturing.

3) Load-bearing and Assistive Integrated Leg Module

The thigh and calf modules have unified functions, serving as support components for transmitting gravitational force downward when stationary and as drive arms for utilizing the body's excess kinetic energy during movement. They are connected via a knee energy storage joint. To accommodate different body sizes, these two modules are connected to the waist-hip and foot modules using adjustable carbon fiber plates with fixed positions.

4) Elastic Energy Storage Knee Joint

The knee joint is the core power-assisting module of the exoskeleton. It utilizes the force exerted by leg muscles on the knee during human walking and running, combined with body weight, to drive the internal energy storage structure, thereby achieving the storage and release of kinetic energy. The knee joint is designed with degrees of freedom in the sagittal plane, and its rotation axis can be adjusted to align with the human knee's bending axis, enabling efficient kinetic energy collection and better alignment with human movement degrees of freedom. This prototype uses a torsion spring as the energy storage component, located on the outer side of the knee joint, with the torsion plane parallel to the sagittal plane. During running, as the leg bends further, the gravitational load is applied to the human body and the knee joint module. As the center of gravity shifts, part of the potential energy is recovered by the torsion spring. The linkage between the exoskeleton components and the torsion spring can be quickly disengaged by removing the internal pins. When soldiers need to perform complex tactical maneuvers, the assistive components can be disengaged to switch movement modes.

5) Replaceable foot module

The foot module primarily serves to bear the gravitational force transmitted from other modules and transfer it to the ground. In the auxiliary load-bearing design, the horizontal distance between the load center of gravity and the ground support point of the foot module is generally between 100 and 200 mm, while the load-bearing mounting height is around 1,400 mm. When a person is standing or walking, most of the load is supported by the foot module. Since the feet frequently absorb impacts during human movement, the foot module is designed with material wear in mind and is engineered as an easily removable and replaceable component.

II. C. 2) Exoskeleton morphology design based on topology optimization

1) Selection of topology optimization objects

When performing topology optimization design on exoskeletons, it is not advisable to perform unified optimization calculations on all components. Therefore, a more efficient design method is to first screen the core components of the product that require optimization design, and then analyze and calculate them one by one. This maximizes the utilization of topology calculation resources and improves optimization accuracy.

2) Setting Topology Optimization Objectives

Clearly define the objectives of the optimization design and accurately set the optimization parameters. The setting of topology optimization parameters must be determined based on different optimization objectives, with the constraints being multi-dimensional. These constraints can be volume-based or force-based. In this study, the load values on the exoskeleton equipment are far below the material's yield strength. Therefore, using volume fraction as the topology optimization objective can effectively achieve lightweight optimization results. However, in product designs where volume constraints are not applicable and stress conditions are extreme, stress extremes should be prioritized as the primary objective of topology optimization.

3) Topology optimization design process

The computational results generated by topology optimization can clearly present the mechanical characteristics of components, providing valuable reference for form design during the conceptual design phase. Therefore, topology optimization serves not only as a design optimization and validation process but also as an auxiliary tool for generating design concept proposals throughout the industrial design process. The design process incorporating topology optimization should be iterative and nonlinear.

4) Topology Optimization Design Results

For exoskeleton equipment design, ergonomic usability and mechanical performance are equally important. Therefore, the styling design of exoskeletons needs to be integrated with engineering design, and topology optimization methods can address this issue [27]. Structural components generated using topology optimization methods are difficult to produce in bulk using traditional subtractive manufacturing methods, while additive manufacturing can handle more complex structural forms.

II. D. Device Size Design

Since the exoskeleton equipment designed in this paper needs to be closely integrated with the soldier's body and work in coordination with it, the dimensions of the locomotion device must be accurately designed according to human body size parameters. However, current human body size parameters are primarily measured in standard standing and sitting postures, with no standard parameters for other postures. Therefore, to obtain the various size parameters of the human body in a semi-prone position, further calculations must be based on the size parameters of the standard standing and sitting postures. According to GB/T 10000, the semi-prone walking posture adopted by exoskeleton equipment does not differ significantly from the standing and sitting postures. As long as all joint angles in the semi-prone posture are determined, the required parameters for the human body in the semi-prone posture can be fully calculated using the dimensional parameters of the standing and sitting postures.

This paper uses programming software to analyze and compare the differences in joint angles between the semi-prone position and the standing and sitting positions. After setting up the calculation program based on all joint angles in the semi-prone position, the human body parameters in the standing and sitting positions are input into the program according to GB/T10000. The final results are summarized to obtain the human body dimensions required for designing a single-soldier wheeled auxiliary walking device in the semi-prone position. The human body dimensions for standing and sitting postures for males aged 18–25 are shown in Tables 1 and 2, respectively.

Table 1: Standing Body Size Table (mm)

Measurement project	Percentile						
	1	5	10	50	90	95	99
1. Eye tall	1452	1479	1497	1585	1658	1653	1712
2. Shoulder height	1255	1274	1302	1353	1426	1462	1509
5. will block the height	704	744	759	805	851	860	889
6. The tibial point is high							

Table 2: Seated Body size table (mm)

Measurement project	Percentile						
	1	5	10	50	90	95	99
9.Eye height	707	758	764	805	841	849	862

10.Shoulder height	531	572	560	598	631	646	659
12.Thigh thickness	95	125	123	128	154	158	160
13.Knee height	446	463	468	499	534	538	558
14.Calf length	369	385	397	419	464	454	477
15.Depth of sitting	403	428	433	467	480	506	520
16.Hip pitch	510	505	520	548	603	592	616

Enter the parameters from the table above into the programming software to obtain the human body dimensions for the semi-prone position. The human body dimensions for the semi-prone position are shown in Table 3.

Table 3: Human size table for semi-prone position (mm)

Measurement project	Percentile						
	1	5	10	50	90	95	99
2.1 Eye height	518	527	530	563	584	608	603
2.2 Chest height	355	352	375	381	391	393	405
2.3 Shoulder height	466	490	493	531	538	549	562
2.4 Hip height	411	411	427	437	450	456	464
2.5 Knee height	134	154	155	164	159	167	160
2.6 Foot heel	211	234	222	232	241	253	250

Based on the aforementioned human body dimension parameters, the height range of 168–180 cm for males was selected, and the preliminary range for the thigh load-bearing rod length of the exoskeleton equipment was determined to be 490 mm–540 mm. the length range for the lower leg load-bearing rods is 400mm to 440mm, the width and length ranges for the chest load-bearing plates are 340mm to 350mm and 420mm to 450mm, respectively, and the length ranges for the folding rod's long and short rods are 530mm to 560mm and 250mm to 280mm, respectively.

II. E. Design of an intelligent sensing system for exoskeletons

II. E. 1) Overview of Intelligent Sensing Systems

The intelligent sensing system is designed to analyze the gait of test subjects wearing AIDER shoes and identify the wearer's movement intentions. The system mainly consists of a posture measurement system and an intelligent shoe system. The block diagram of the intelligent sensing system is shown in Figure 3.

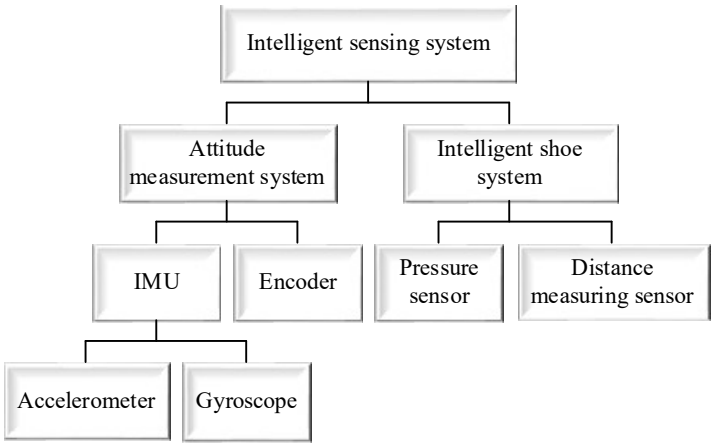

Figure 3: Block diagram of the intelligent sensing system structure

The posture measurement system primarily consists of an IMU measurement unit and an encoder. The IMU measurement unit is mounted on the back of AIDER, with its primary function being to measure the three-dimensional posture and movement speed of AIDER's torso during walking. By measuring the three-dimensional spatial angles of AIDER using the IMU measurement unit and combining them with predefined thresholds, it is possible to monitor whether AIDER's movements are normal. Encoders are installed at three joints of AIDER, used to measure the angular rotation of AIDER's joints during walking. This information can also serve as reference data for motor control. The exoskeleton intelligent shoe system primarily consists of pressure sensors and distance

sensors. The pressure sensors are embedded in the sole of the intelligent shoe to measure the interaction force between AIDER's foot and the ground during walking. The distance sensors are installed on the outer side of AIDER's lower leg linkage to measure the distance between AIDER's shoe tip and the obstacle ahead, as well as the distance between AIDER's foot sole and the ground. Sensor selection, circuit design, mechanical design, and software functionality implementation are the main components of this system's design [28]. Sensor selection is the first step in this system. To successfully complete the overall sensor system platform, it is also necessary to design and implement the electronic circuit hardware components that enable sensor functionality. During the hardware design process, mechanical design must also be coordinated to ultimately complete sensor selection, circuit design, and mechanical design, thereby achieving the establishment of the intelligent sensor system platform.

II. E. 2) Sensor Solution Determination

Analyzing the walking gait of exoskeleton robots not only helps exoskeleton robots adjust their movement states based on specific actual conditions to ensure system safety but also reflects the wearer's recent health status through gait data analysis. The walking trajectory of the foot is calculated using an IMU, and then the stride length and step height parameters are calculated. The advantage of this approach is that the IMU is not affected by external interference. However, this approach also has shortcomings, namely cumulative error in the IMU. To address this issue, a specific reference benchmark can be used to reduce the error. For example, the zero-speed update method can be adopted, where the IMU data is updated when the foot velocity is zero, significantly reducing the cumulative error in the IMU during the calculation process. To ensure the stability of the exoskeleton robot's walking, two six-degree-of-freedom force/torque sensors are used to measure the forces between the exoskeleton robot's foot and the ground, and then the foot's center of pressure (CoP) coordinates are calculated based on stability theory. However, this type of sensor is expensive. This paper selects a single-degree-of-freedom pressure sensor, which is cost-effective, compact, and offers a high overall performance-to-cost ratio. Motion intent recognition is a key focus of this study. By identifying the wearer's motion intent, the exoskeleton robot's overall walking process can be made smoother, while also significantly improving the wearer's comfort. In this study, an IMU measurement unit is designed using inertial sensors (accelerometers and gyroscopes), and combined with data from the smart shoe system to identify the wearer's motion intent.

II. E. 3) Overall Circuit Structure Design

The overall block diagram of the electronic circuit for the intelligent sensing system is shown in Figure 4. The microprocessor serves as the core of the entire circuit. The accelerometer and gyroscope form the IMU measurement unit, while the pressure sensor and distance sensor are the primary sensor components of the intelligent shoe. The IMU and intelligent shoe are connected to the main controller via a CAN bus. Additionally, both the IMU and intelligent shoe can communicate with a PC via a serial port or wireless module, facilitating real-time data display and analysis during the initial R&D phase. The SWD port is retained to facilitate program debugging during the R&D phase, thereby improving R&D efficiency. Additionally, to enhance the circuit's functionality, other input/output devices such as buttons and LED lights are also included.

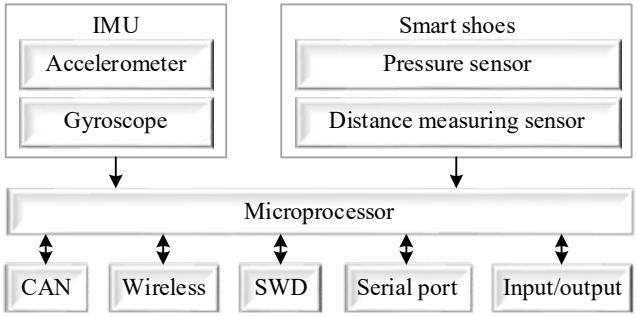

Figure 4: Overall framework of the circuit

II. E. 4) Mechanical Design and Implementation

The structural design of AIDER incorporates biomimetic principles, with adjustments made to certain components to ensure usability and safety. Each leg of AIDER has three degrees of freedom, with two motors installed at the hip and knee joints to provide power, while the ankle joint uses a spring-driven passive motion mechanism. Absolute encoders are installed at each joint to measure the rotational angles during walking. Pressure sensors are installed in the sole of the AIDER smart shoe to measure the force between the AIDER's foot and the ground. IMU sensors

are installed at the hip and on the smart shoe to measure the AIDER's three-dimensional posture during walking. An infrared sensor is installed on the outer side of the ankle joint to measure the distance between the AIDER and obstacles ahead, as well as the distance between the AIDER's foot and the ground during walking. The smart shoe is an important component of the sensor system. The mechanical structure of the smart shoe consists of two layers: an upper metal layer and a lower rubber layer. The metal layer is divided into front and rear sections, connected by a hinge. This structure ensures that pressure is effectively transmitted to the sensors while maintaining the integrity of the overall structure, and also improves comfort during walking. The lower rubber layer is designed with countersunk holes for housing sleeves. One end of the sleeve is sealed, with the pressure sensor inverted inside the sleeve and then embedded into the rubber countersunk hole. Since the pressure sensor's pressure head is a very small point, if directly embedded in the rubber countersunk hole, the pressure head would be pressed into the rubber during walking and fail to achieve the desired pressure measurement effect. Therefore, the sleeve design is necessary. The other end of the pressure sensor is connected to the metal layer of the smart shoe via screws. The metal layer is connected to the rubber layer via rivets, with the rivet bases embedded within the rubber. This prevents the rivets from directly contacting the ground, thereby improving walking comfort.

III. Results and discussion

III. A. Simulation Experiment

III. A. 1) Human-machine motion area compatibility analysis

The changes in hip and knee joint angles are shown in Table 4. The thigh length ranges from 400 to 550 mm, and the calf length ranges from 340 to 450 mm. To validate the rationality of the lower limb rehabilitation exoskeleton design, using the exoskeleton's end effector as a reference, a single human gait cycle was selected. The joint input data of the exoskeleton were used to perform kinematic analysis of the exoskeleton using MATLAB. Using the ankle joint walking trajectory of the human model as a reference, the compatibility between the ankle joint walking region of the lower limb exoskeleton and the ankle joint walking trajectory of the human body was verified. The human-machine motion region compatibility analysis is shown in Figure 5. From this, it can be concluded that the range of motion of the exoskeleton ankle joint is similar to that of the human ankle joint. The walking space designed for the lower limb exoskeleton within the sagittal plane can cover the walking trajectory of the human ankle joint, meeting the requirements of human kinematics.

Table 4: Changes in the angles of the hip and knee joints

Time/s	0	0.1	0.2	0.3	0.4	0.5	0.6	0.7	0.8	0.9	1	1.1	1.2
Knee joint/(°)	22.95	20.04	11.49	5.16	11.01	33.45	67.38	69.81	43.70	5.16	8.58	16.87	21.03
Hip joint/(°)	22.73	12.48	-2.88	-11.43	-15.10	-10.95	5.64	22.73	27.37	28.33	28.59	26.86	21.26

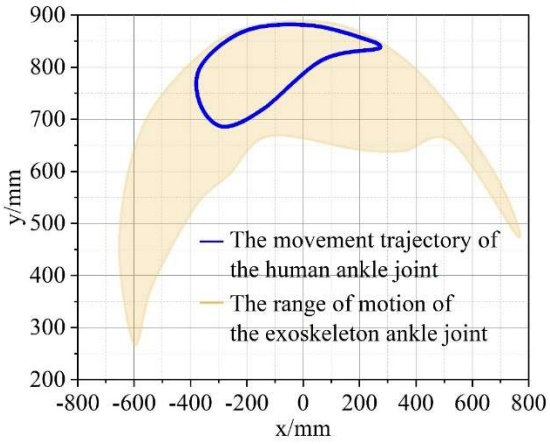

Figure 5: Compatibility analysis of human-machine motion areas

III. A. 2) Human-machine dynamics simulation

The exoskeleton is equipped with motion capture sensors on the feet, calves, thighs, and waist. These sensors are 9-degree-of-freedom inertial sensors, comprising accelerometers, gyroscopes, and magnetometers, and are fitted with batteries and Bluetooth transmitters to detect human posture during movement. Using the motion capture sensors, joint data is measured for various human movement states. After obtaining the data, simplified models of

the human body and exoskeleton are created in simulation software. The materials for each component of the exoskeleton model are set. The materials for the exoskeleton components are aluminum, the ground material is rubber, and the limb model material is human tissue. A dynamic simulation is performed on the exoskeleton model to simulate its dynamic characteristics, yielding the magnitude of the driving torque at each joint. By comparing joint data with and without the exoskeleton, the effectiveness of the exoskeleton is validated. Based on the weight and rotational inertia of the human lower limbs, the material properties of each component are increased. In the graphical part list, select the parts to be edited and edit the mass information of each part individually.

After software simulation, the values of spring deformation over time in the human-machine dynamics model are obtained. The relationship between spring deformation and phase is shown in Table 5. By overlaying the human gait phase diagram with the spring deformation curve diagram, it can be observed that the spring begins to store energy when entering the support phase, reaches its peak energy storage during the latter part of the support phase, and rapidly releases energy during the foot-off phase, returning to its original length. This validates the correctness of the design principle.

Table 5: The relationship between the deformation of the spring

Time/s	0	0.1	0.2	0.3	0.4	0.5	0.6	0.7	0.8	0.9	1	1.1	1.2
Spring formation/mm	-0.55	0.98	0.98	9.81	13.91	48.96	50.48	53.54	67.50	70.73	16.13	3.19	0.80

In the dynamic simulation analysis of lower limb exoskeletons, removing additional components such as energy-storage springs allows us to obtain the torque curves of the knee and ankle joints when the lower limb exoskeleton is not worn. The comparisons of knee and ankle joint torque between wearing and not wearing the lower limb exoskeleton during walking are shown in Figures 6 and 7, respectively. Overall, compared to not wearing the exoskeleton, wearing the exoskeleton results in an increase in knee joint torque and a significant decrease in ankle joint torque. Therefore, it can be concluded that the lower limb assistive exoskeleton provides significant assistance at the ankle joint.

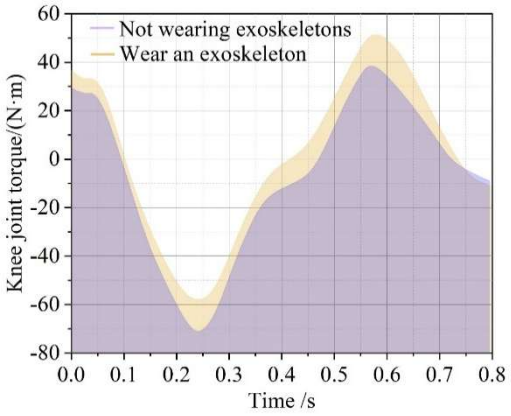

Figure 6: Torque of the walking knee joint

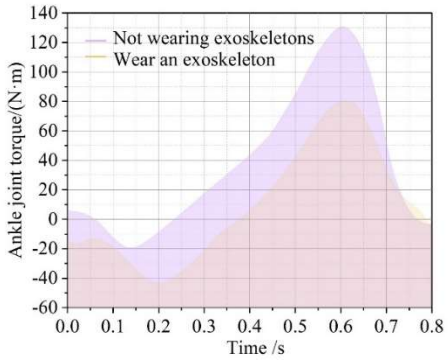

Figure 7: Ankle joint torque when walking

Through simulation, the power curves of the knee and ankle joints without wearing lower limb exoskeletons can be obtained. The comparisons of the power of the knee and ankle joints with and without wearing lower limb exoskeletons are shown in Figures 8 and 9, respectively.

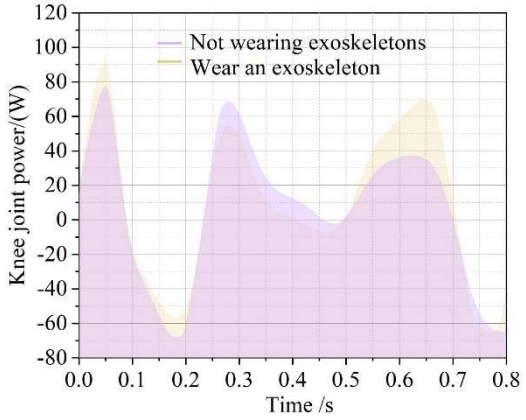

Figure 8: Walking knee joint power

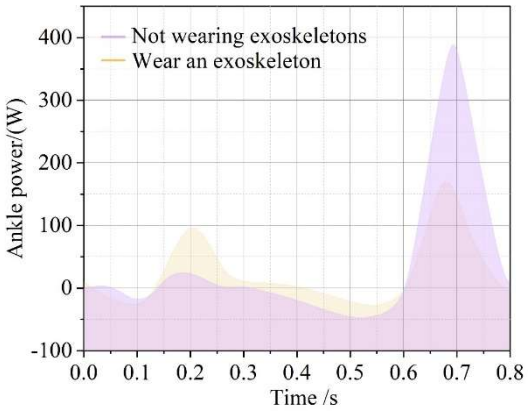

Figure 9: Walking ankle joint power

By integrating joint power over time, we can determine the work done by the knee and ankle joints during walking, both with and without wearing an exoskeleton. The work values for walking with and without an exoskeleton are shown in Table 6. When wearing an exoskeleton, the work done by the knee joint increases, while the work done by the ankle joint decreases, with a significant reduction in the latter. By summing the work done by both joints, it can be concluded that the total work done by the lower limb joints is significantly reduced when wearing an exoskeleton, with a reduction percentage of 20.71%. This confirms that the assistive exoskeleton has a significant effect.

Table 6: The work value of walking exercise

Lower limb joint	No work in outer bones/J	The amount of work in outer bones/J	Difference/J
Knee joint	28.0185	30.31	-2.2915
Ankle joint	49.0565	30.8023	18.2542
Total amount	77.075	61.1123	15.9627
Reduce the percentage		20.71%	

The comparison of knee and ankle joint torques between wearing an exoskeleton and not wearing an exoskeleton during squat exercises is shown in Tables 7 and 8, respectively. Overall, wearing an exoskeleton resulted in a reduction in knee joint torque and a significant reduction in ankle joint torque compared to not wearing an exoskeleton.

Table 7: Knee joint torque when squatting and standing up

Time/s	0	0.5	1	1.5	2	2.5
Not wearing exoskeletons(N·m)	-7.01	31.66	107.64	80.07	16.21	-4.67
Wearing exoskeletons(N·m)	-7.68	27.62	101.58	76.03	8.80	-8.04

Table 8: Ankle joint torque when squatting

Time/s	0	0.51	1.02	1.53	2.04	2.55
Wearing exoskeletons(N·m)	-5.95	-8.46	-1.97	-10.87	-8.34	-2.21
Not wearing exoskeletons(N·m)	-6.30	-23.83	-27.68	-34.64	-16.51	-2.69

The simulation results for the power output of the knee and ankle joints with and without exoskeletons are shown in Tables 9 and 10.

Table 9: Ankle joint power when squatting and standing up

Time/s	0	0.5	1	1.5	2	2.5
Wearing exoskeletons(W)	-1.70	-8.33	-0.50	9.19	7.67	1.20
Not wearing exoskeletons(W)	-1.36	-22.28	-12.07	27.91	12.61	1.20

Table 10: Knee joint power during squatting and standing

Time/s	0	0.5	1	1.5	2	2.5
Wearing exoskeletons(W)	10.96	-53.70	-87.74	121.88	18.38	-1.99
Not wearing exoskeletons(W)	8.87	-61.21	-96.62	138.90	25.90	2.08

By calculating the integral, the work done by the knee and ankle joints during squatting movements can be determined when wearing an exoskeleton and when not wearing an exoskeleton. The work values for squatting movements with and without an exoskeleton are shown in Table 11. When wearing an exoskeleton, the work done by both the knee and ankle joints decreases. By adding the work done by both joints, it can be determined that the total work done by the lower limb joints during squatting movements is significantly reduced when wearing an exoskeleton, with a reduction percentage of 17.57%. .

Table 11: The work value of squatting and standing exercises

Lower limb joint	No work in outer bones/J	The amount of work in outer bones/J	Difference/J
Knee joint	150.9395	139.7899	11.1496
Ankle joint	37.5158	15.5522	21.9636
Total amount	188.4553	155.3421	33.1132
Reduce the percentage		17.57%	

III. B. Sensor System Data Acquisition and Gait Condition Recognition

The experimental data collector recorded sensor sampling data for the left lower limb joint angles over a 20-second period, from standing—walking on flat ground—ascending stairs—descending stairs—walking on flat ground. The identification of gait conditions (standing, walking on flat ground, ascending stairs, and descending stairs) first requires dividing the collected sample data into multiple sample segments, with each segment representing a complete gait. The segmentation criteria must ensure uniqueness within a single gait while also being applicable to all target terrain conditions. As shown by the curve of the combined plantar pressure force, the transition from pressure presence to absence (when no pressure is applied, the output of the 11 plantar sensors on the sole is approximately 0.8V) during flat walking, ascending stairs, and descending stairs meets the segmentation criteria for sample segments. Standing can be considered as foot pressure lasting for more than 4 seconds, and then processed in 2-second sample segments. After selecting the sample segments, it is necessary to select feature values that can distinguish these typical road conditions within the sample segments. The average and standard deviation of the hip joint, knee joint, and ankle joint angle data within the sample segments were selected as feature values for comparison and analysis. Comparative studies found that ankle and knee joint angle feature values are

difficult to distinguish between the four common road conditions, but hip joint feature values can effectively distinguish between standing, walking on flat ground, ascending stairs, and descending stairs. Therefore, hip joint feature values were selected for further research. The statistical results of gait recognition are shown in Table 12. It can be seen that this method achieves high accuracy in recognizing ascending stairs, walking on flat ground, and standing, but there is room for improvement in recognizing descending stairs. The primary reason is the insufficient number of training samples, with unrecognized points and new road conditions (such as turning steps and road condition transition steps) significantly affecting the recognition accuracy.

Table 12: The Results Statistics of Gait Recognition

Sample eigenvalue road conditions	standing	Upstairs ladder	Stair ladder	gradation	Unidentified point	Recognition rate(%)
standing	17	0	0	0	0	100
Upstairs ladder	0	33	0	0	2	94.29
Stair ladder	0	1	25	0	3	86.21
gradation	0	0	0	106	9	92.17
New road	5	0	0	0	4	55.56
Identification number	22	34	25	106	18	91.22

III. C. Performance evaluation experiments

This section conducts performance evaluation tests. Seven evaluation experiments were conducted, and the experimental data was calculated using the lower limb exoskeleton robot performance evaluation calculation model. The arithmetic mean of the calculation results was then calculated.

III. C. 1) Analysis of prototype comfort evaluation results

The scores for each comfort indicator in the 7 experiments are shown in Figure 10. As can be seen from the score chart in Figure 7, all indicators in the comfort evaluation of the prototype scored above 80 points. Among them, the comfort scores for the lining material and waist operation of the prototype both reached above 85 points, indicating that the selection of the lining material is appropriate and the waist operation is comfortable with no sense of constraint. While the thigh operation comfort and color comfort also achieved good rating results, their scores were around 80 points, indicating room for improvement. Observing the scoring trends of each evaluation indicator over seven trials reveals that as the number of experiments increases, the scores for color, design, lining material, and surface material comfort tend to stabilize, while the scores for waist and thigh comfort slightly decrease. This indicates that under prolonged wear, the comfort of the waist and thighs diminishes.

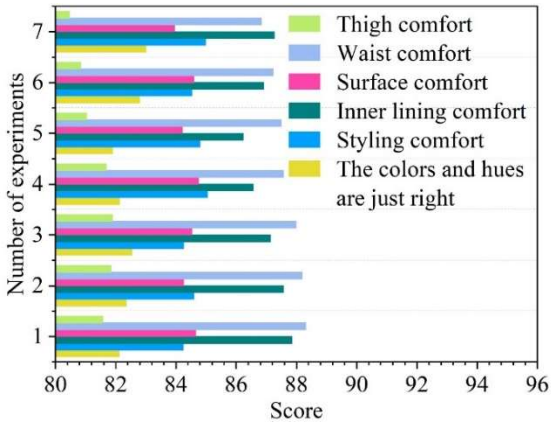

Figure 10: The scores of each secondary evaluation index of comfort

III. C. 2) Analysis of prototype functional evaluation results

The scores for the functional evaluation of the prototype are shown in Figure 11 (Figure a shows the scores for environmental adaptability indicators in seven experiments, and Figure b shows the scores for other functional indicators in seven experiments). As shown in the line chart of scores from the 7 experiments in Figure (a), the scores for all environmental adaptability evaluation indicators of the prototype, except for obstacle crossing, remained stable between 70 and 80 points, indicating that the overall environmental adaptability of the prototype is average. Among these, the prototype achieved scores of around 78 points for adaptability in flat terrain at both fast

and slow speeds, descending stairs, and ascending/descending slopes, demonstrating that the prototype has good adaptability to flat terrain, slopes, and stair environments. The scores for climbing stairs and crossing ditches are around 72 points, indicating that in environments such as crossing ditches and climbing stairs, the prototype's range of motion slightly restricts the user's own movement. However, during obstacle crossing, the prototype's adaptability score is below 70 points, proving that the prototype is not suitable for obstacle crossing and requires redesign based on the physiological joint angles of the human body during obstacle crossing. As shown in Figure (b) 7 experimental score line chart, the prototype's convenience evaluation scores are above 80, indicating that the process of wearing, operating, and removing the prototype is relatively convenient. As the number of experiments increases, the three convenience evaluation scores show a slight upward trend, indicating that as familiarity increases, the convenience scores slightly increase. The prototype's scores for assistive performance and wearing fatigue are between 70 and 80 points, indicating that the prototype's assistive performance is average and prolonged wearing does not reduce muscle fatigue. As the number of experiments increases, the average scores for standing assistive performance, walking assistive performance, and muscle fatigue all show a decreasing trend, indicating that prolonged wearing reduces the perceived assistive performance and increases wearing fatigue.

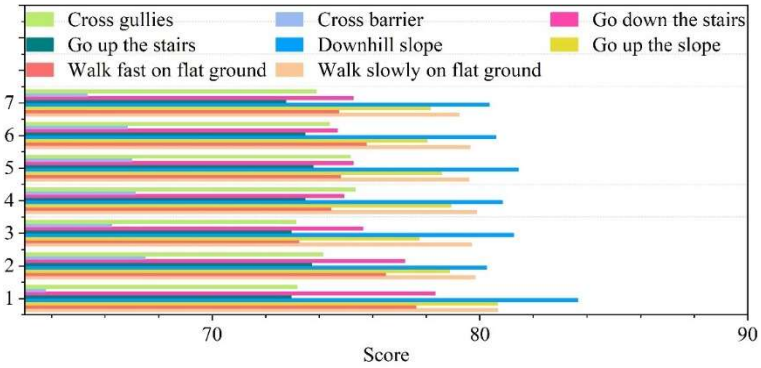

(a) The scores of the secondary evaluation index

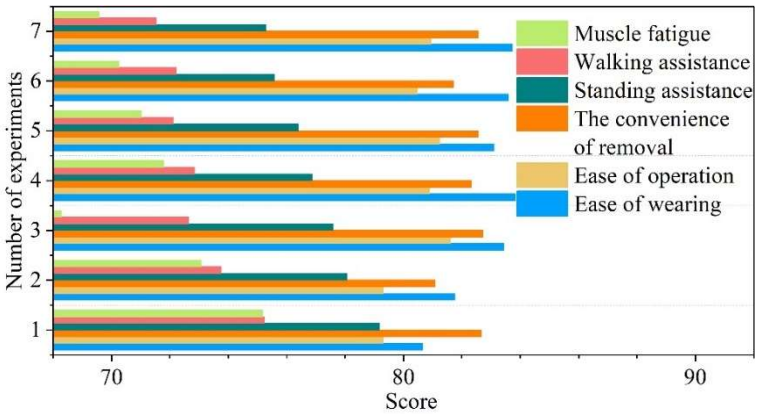

(b) Scores were obtained for other secondary evaluation indicators

Figure 11: The score in the functional evaluation

IV. Conclusion

This paper designs the human-machine interaction and product design of an exoskeleton smart wearable device. Through a series of experiments, the feasibility and effectiveness of the designed product are validated.

Through dynamic simulation experiments, it was found that after wearing the exoskeleton, the total work done by the joints during walking and squatting movements decreased by 20.71% and 17.57%, respectively.

Additionally, gait recognition simulation results demonstrated the rationality and feasibility of the military exoskeleton sensor system designed in this paper.

In the prototype comfort evaluation, all indicators scored above 80 points, with the lining material comfort and waist operation comfort scores both exceeding 85 points. This confirms that the selected lining material is appropriate and the waist operation is comfortable.

Funding

This work was supported by National Natural Science Foundation of China (Grant No. 52201385).

References

[1] Lu, L., Zhang, J., Xie, Y., Gao, F., Xu, S., Wu, X., & Ye, Z. (2020). Wearable health devices in health care: narrative systematic review. JMIR mHealth and uHealth, 8(11), e18907.

[2] Cheng, J. W., & Mitomo, H. (2017). The underlying factors of the perceived usefulness of using smart wearable devices for disaster applications. Telematics and Informatics, 34(2), 528-539.

[3] Yen, H. Y., Liao, Y., & Huang, H. Y. (2022). Smart wearable device users' behavior is essential for physical activity improvement. International Journal of Behavioral Medicine, 29(3), 278-285.

[4] Koutromanos, G., & Kazakou, G. (2020). The Use of Smart Wearables in Primary and Secondary Education: A Systematic Review. Themes in eLearning, 13, 33-53.

[5] Nunes, G. S., & Arruda Filho, E. J. M. (2018). Consumer behavior regarding wearable technologies: Google Glass. Innovation & Management Review, 15(3), 230-246.

[6] Radnejad, A. B., Ziolkowski, M. F., & Osiyevskyy, O. (2021). Design thinking and radical innovation: enter the smartwatch. Journal of Business Strategy, 42(5), 332-342.

[7] Stolz, K., Heyder, T., Gloor, P. A., & Posegga, O. (2019). Measuring Human-Animal Interaction with Smartwatches: An Initial Experiment. Collaborative Innovation Networks: Latest Insights from Social Innovation, Education, and Emerging Technologies Research, 165-182.

[8] Polley, C., Jayarathna, T., Gunawardana, U., Naik, G., Hamilton, T., Andreozzi, E., ... & Gargiulo, G. (2021). Wearable bluetooth triage healthcare monitoring system. Sensors, 21(22), 7586.

[9] Huang, C., & Kelly, J. (2022). Toward better posture: a wearable back posture alerting device. Journal of Student Research, 11(2), 1-15.

[10] Mencarini, E., Rapp, A., Tirabeni, L., & Zancanaro, M. (2019). Designing wearable systems for sports: a review of trends and opportunities in human–computer interaction. IEEE Transactions on Human-Machine Systems, 49(4), 314-325.

[11] Zhou, H., Gao, Y., Song, X., Liu, W., & Dong, W. (2019). Limbmotion: Decimeter-level limb tracking for wearable-based human-computer interaction. Proceedings of the ACM on Interactive, Mobile, Wearable and Ubiquitous Technologies, 3(4), 1-24.

[12] He, S., Tung, W. F., & Lin, S. L. (2024). Analysis of User Experience of Hand Gestures for Interaction with Wearable Devices. International Journal of Human–Computer Interaction, 40(16), 4252-4264.

[13] Kutilek, P., Volf, P., Viteckova, S., Smrcka, P., Krivanek, V., Lhotska, L., ... & Stefek, A. (2017, May). Wearable systems for monitoring the health condition of soldiers: Review and application. In 2017 International Conference on Military Technologies (ICMT) (pp. 748-752). IEEE.

[14] Lo, M., Carstairs, G., Mudie, K. L., Begg, R., & Billing, D. (2020). The use of wearable assistive technology to increase soldiers' effectiveness. Human Factors and Mechanical Engineering for Defense and Safety, 4, 1-8.

[15] Kodam, S., Bharathgoud, N., & Ramachandran, B. (2020). A review on smart wearable devices for soldier safety during battlefield using WSN technology. Materials Today: Proceedings, 33, 4578-4585.

[16] Korpela, C., & Walker, A. (2018, August). Wearable technologies for enhanced soldier situational awareness. In Proceedings of the 2nd International Conference on Vision, Image and Signal Processing (pp. 1-6).

[17] Gaikwad, N. B., Khare, S. K., Ugale, H., Mendhe, D., Tiwari, V., Bajaj, V., & Keskar, A. G. (2023). Hardware Design and Implementation of Multiagent MLP Regression for the Estimation of Gunshot Direction on IoBT Edge Gateway. IEEE Sensors Journal, 23(13), 14549-14557.

[18] Bilir, M. Z., & Gürcüm, B. H. (2018). Ballistic wearable electronic vest design. Journal of Industrial Textiles, 47(7), 1769-1790.

[19] Shi, H., Zhao, H., Liu, Y., Gao, W., & Dou, S. C. (2019). Systematic analysis of a military wearable device based on a multi-level fusion framework: research directions. Sensors, 19(12), 2651.

[20] Singh, R. K., & Mishra, S. (2024). EM Trigger Defender Glove: A Next-Gen IoBT Solution for Soldier Protection. IEEE Sensors Letters.

[21] Almer, A., Weber, A., Paletta, L., Schneeberger, M., Ladstätter, S., Wallner, D., ... & Hölzl, T. (2021). Multisensory wearable vital monitoring system for military training, exercise and deployment. In Advances in Neuroergonomics and Cognitive Engineering: Proceedings of the AHFE 2021 Virtual Conferences on Neuroergonomics and Cognitive Engineering, Industrial Cognitive Ergonomics and Engineering Psychology, and Cognitive Computing and Internet of Things, July 25-29, 2021, USA (pp. 497-505). Springer International Publishing.

[22] Mhatre, T., Mali, Y., Chaudhari, S., Ganorkar, M., & Dahalke, P. (2020). Design of Shoes Against Landmines. INTERNATIONAL JOURNAL OF ENGINEERING RESEARCH & TECHNOLOGY (IJERT), 9(09).

[23] Jia-Yong, Z., Ye, L. I. U., Xin-Min, M. O., Chong-Wei, H. A. N., Xiao-Jing, M. E. N. G., Qiang, L. I., ... & Ang, Z. H. A. N. G. (2020, March). A preliminary study of the military applications and future of individual exoskeletons. In Journal of Physics: Conference Series (Vol. 1507, No. 10, p. 102044). IOP Publishing.

[24] Schnieders, T. M., Stone, R. T., Oviatt, T., & Danford-Klein, E. (2017). ARCTiC LawE: An Upper-Body Exoskeleton for Firearm Training. Augmented Human Research, 2, 1-10.

[25] Pui Wah Kong,Ang Hong Koh,Mei Yee Mavis Ho,Muhammad Nur Shahril Iskandar & Cheryl Xue Er Lim. (2024). Effectiveness of a passive military exoskeleton in off-loading weight during static and dynamic load carriage: A randomised cross-over study.. Applied ergonomics,119,104293-104293.

[26] Man Bok Hong,Gwang Tae Kim & Yeo Hun Yoon. (2019). ACE-Ankle: A Novel Sensorized RCM (Remote-Center-of-Motion) Ankle Mechanism for Military Purpose Exoskeleton.Robotica,37(12),2209-2228.

[27] Slocombe Geoff. (2015). Military exoskeletons: Heavier loads, faster and for longer. Asia-Pacific Defence Reporter (2002),41(7),34-35.

[28] Gruevski Kristina M,Cameron Ian J,McGuinness Cerys,Sy Adrienne,Best Krista L,Bouyer Laurent... & Karakolis Thomas. (2021). A pilot investigation of the influence of a passive military exoskeleton on the performance of lab-simulated operational tasks.. IISE transactions on occupational ergonomics and human factors,8(4),11-10.